



Synthesis and characterization of novel mixed complexes derived from 2-aminomethylbenzimidazole and 2-(1*H*-benzimidazol-2-yl) aniline and theoretical prediction of toxicity



Lotfi Mohamed Aroua^{a*,b}

^{a*} Department of Chemistry, College of Science, Qassim University, Campus University, King Abdulaziz Road, Al-Malida, 51452 - P.O.Box: 6644, Buraydah, Qassim, Kingdom Saudi Arabia.

^b Laboratory of Organic Structural Chemistry & Macromolecules, Department of Chemistry, Faculty of Sciences of Tunis, Tunis El-Manar University, El Manar I 2092, Tunis Tunisia.

Abstract: Novel complex derived from 2-aminomethylbenzimidazole, 2-(1*H*-benzimidazol-2-yl) aniline and metal chloride (Cd (II), Ni(II) and Cu(II)) was successfully synthesized. All newly complexes were fully characterized by spectroscopic data of FT-IR, UV-Visible electronic absorption, X-ray powder diffraction, and thermal analysis. IR spectra of the metal complexes revealed the coordination of the ligands to the metal ions via nitrogen atoms and mass spectra proposed that have a tetrahedral structure. The X-ray powder diffraction results affirmed that the Cu (II) complex has a triclinic structure, Cd (II) complex possess a triclinic structure and Ni (II) complex occupy a rhombohedral structure. The bioactivity score of tested compounds possesses a similar as compared to aspirin for all drug targets. The results of the theoretical toxicity study of different new complexes have been achieved based on program protox-II-prediction toxicity of chemicals and revealed that all target compounds exhibited no significant toxicity to all human cells.

Keywords: Mixed complex, 2-aminomethylbenzimidazole, 2-benzimidazole aniline, spectral studies, XRD analysis, thermal stability, theoretical prediction of toxicity.

1. Introduction

Benzimidazole nucleus is an extraordinary structure that exhibits extensive biological and therapeutic activity. In previous years, the research describing the importance of systems containing benzimidazole heterocyclic system was largely multiplied and covered vast bioactive activities including antimicrobial [1-3], antifungal [4], anti-inflammatory [5,6] antihelminthic [7], antitubercular [8,9], antithrombotic; antiplatelet and anticoagulant [10], antiulcer [11], antiprotozoal [12], antileishmanial [13], anti-inflammatory [14], antiviral [15]

antimycobacterial [16], anti-HIV [17], antitumour [18].

Recently, benzimidazole target was reported as an anti-hypertensive agent [19, 20], potent non-nucleoside reverse transcriptase inhibitors [21], inhibitors of the hepatitis C virus [22], anticonvulsant [23], ulcerogenic [24], nonpeptide angiotensin II receptor antagonists [25], potent activators of AMP-activated protein kinase [26] and antileukemic agents [27]. R.V. Shingalapur et al. mentioned that the benzimidazole core is used with good efficiency for the treatment of tuberculosis [28]. Furthermore,

*Corresponding author e-mail: lm.aroua@qu.edu.sa, aroua.lotfi@yahoo.com

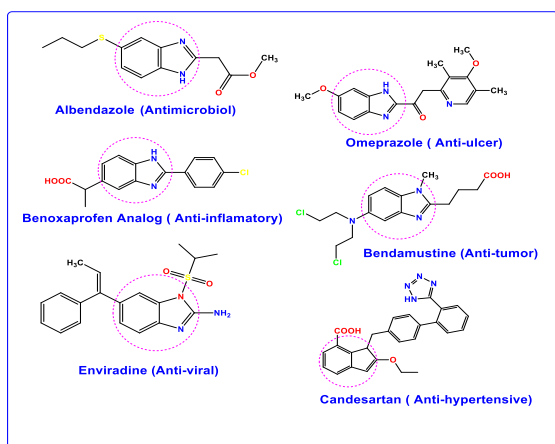
Receive Date: 21 February 2020, Revise Date: 30 March 2020, Accept Date: 17 May 2020

DOI: 10.21608/EJCHEM.2020.24418.2453

©2020 National Information and Documentation Center (NIDOC)

benzimidazole scaffolds were reviewed as anti-cancer agents in the diverse report [29,30].

As a result, several drugs derived from the benzimidazole system have been introduced into the market include omeprazole (Anti-ulcer), Albendazole (antimicrobial), Benoxaprofen Analog (Anti-inflammatory), Bendamustine (Anti-tumor), Envirodine (Anti-viral), Candesartan (Anti-hypertensive) [31] (Fig 1).



On the other hand, the benzimidazoles core finds several applications, especially, widely applied as ligands in the preparation of metal complex. Among, a variety of benzimidazole complexes were investigated and exhibited various important biological activities including antibacterial [32], antifungal [33], antioxidant activity against DPPH and antidiabetic activity against α -amylase [34], antiameobic [35], Potent inhibition of protein tyrosine phosphatases [36] and antimalarial [37].

Furthermore, 2-aminomethylbenzimidazole was considered an intermediate key toward the synthesis of diversely metal complexes possessing therapeutic potential covering antimicrobial and antitumor [38], anti-inflammatory [39], antifungal [40], antitumor [41]. The mixed complex of Cu (II), Ni(II), Zn(II) and Cd(II) ions involving 2-aminomethylbenzimidazole and glycine have been screened for their antifungal and antibacterial activities.

In addition, 2-(1*H*-benzimidazol-2-yl) aniline represent one of the most targeted moieties possessing a wide range of application in different fields. In particular, complex derived from 2-benzimidazole aniline is well-reviewed in medicinal chemistry as antibacterial [42].

Anup Paul et al described for the first time that Schiff base metal complexes derived from 2-(2-aminophenyl)-1*H*-benzimidazole reveal significant anticancer activities [43]. Later, his reported the synthesis of new benzimidazole based Schiff base copper (II) complexes and the biological evaluation showed a higher cytotoxic effect than cisplatin on lung cancer (A-549) cell line [44]. 2-(2-aminophenyl)-1*H*-benzimidazole Schiff base complex was found also a variety of applications in luminescence chemistry as chemosensors [45, 46].

In our pursuit to develop and discover a novel molecular architecture possessing biological activities, we report the synthesis a new series of mixed metal complex Cu(II), Ni(II) and Cd(II) derived from 2-(1*H*-Benzimidazol-2-yl) aniline as ligand **L1** and 2-aminomethylbenzimidazole as ligand **L2**.

2. Experimental

Material and Methods

FT-IR spectroscopy was recorded using the Thermo-Nicolet-6700 FT-IR spectrometer by the KBr disc technique in the wavenumber range of 400-4000 cm^{-1} . Electronic absorption spectral was carried out in DMSO on a UV-2102 PC Shimadzu spectrophotometer using 1 cm matched quartz cell in the wavelength range 200-900 nm. Simultaneous TGA and DTA analyses were performed employing a Shimadzu DTG-60 instrument using a heating rate of 10 $^{\circ}\text{C}/\text{min}$ in air atmosphere. The average sample weight was 10 mg $\alpha\text{-Al}_2\text{O}_3$ was used as reference material in the DTA measurements. The X-ray powder diffraction patterns of the compounds were recorded as an XRD diffractometer Model PW 1710 control unit (Philips). The anode material was Cu K α ($\lambda = 1.54180 \text{ \AA}$), 40 K.V 30 M.A Optics: Automatic divergence slit. All reagents employed in the synthesis of different complexes were commercially available without purification. 2-(1*H*-Benzimidazol-2-yl) aniline and 2-aminomethylbenzimidazole were purchased from sigma-aldrich. The mass spectra of different complexes are registered in a positive mode using the DART-TOF-MS. Two to five of the most intense fragment ions resulting from cleavage possible from the compounds detected were chosen and analyzed. The high-resolution mass spectrometer instrument was AccuTOF LC-Plus from JEOL (Japan).

Preparation of mixed cadmium complex Cd[(L1)(L2)] (1)

To a solution of cadmium Chloride (1.54 g, 8.4 mmol) in 10 mL of ethanol was added a solution of 2-(1*H*-benzimidazol-2-yl) aniline (1.75g, 8.4 mmol) in 10mL of ethanol. The reaction mixture was stirred at room temperature for 30 min and then a solution of 2-aminomethylbenzimidazole (1.23g, 8.4 mmol) in 10 mL of ethanol was added to the mixture and heated under reflux for 4 h. The progress of reaction was controlled with TLC (DMF/ethanol: 20/80). At the end of the reaction, the reaction mixture was cooled, filtered and the residue washed with ethanol and then with DMF to obtain a white precipitate. Mp: 233°C, (85% yield), UV-Vis (DMSO); λ_{\max} [nm]: 287; 353. IR (KBr, ν /cm⁻¹): = 3379 (m), 3174 (m), 3267 (m), 1609 (s), 1530 (s), 1488(m), 1480 (s), 1440 (m), 1402 (s), 1323 (m), 1263 (m), 1156 (m), 1030 (m), 1004 (m), 926 (s), 827(m), 794 (m), 744 (m), 585 (m). 560 (m), 519 (m), 435 (m). HRMS (DART-TOF-MS, positive mode) $m/z = (M+H)^+$: 414.30206, 382.22057, 342.20964, 314.13138, 279.16197, 238.16268, 210.10052, 182.08304, 151.02056, 133.04748, 103.97504.

Preparation of mixed nickel complex [Ni(L1)(L2)] (2)

To a solution of nickel chloride (1.08 g, 8.4 mmol) in 10 mL of ethanol was added a solution of 2-(1*H*-benzimidazol-2-yl) aniline (1.75g, 8.4 mmol) in 10mL of ethanol. The reaction mixture was stirred at room temperature for 30 min and then a solution of 2-aminomethylbenzimidazole (1.23g, 8.4 mmol) in 10 mL of ethanol was added to the mixture and heated under reflux for 4 h. The progress of reaction was controlled with TLC (DMF/ethanol: 20/80). At the end of the reaction, the reaction mixture was cooled, filtered and the residue washed with ethanol and then with DMF to obtain a green precipitate. Mp: > 350°C, (88% yield) , UV-Vis (DMSO); λ_{\max} (nm) : 288, 352. IR (KBr, ν /cm⁻¹): 3285 (m), 3240 (m), 3052(m), 2902 (s), 1571 (s), 1536 (s), 1486 (m), 1442 (s), 1411 (s), 1318 (s), 1280 (s), 1230 (s), 1029 (s), 974 (m), 906 (m), 861 (m), 835 (m), 795(m), 775(m), 693(m), 516(m) 493(m), 435(m). HRMS (DART-TOF-MS, positive mode) $m/z = (M+Na)^+$: 490.04405, 459.22685, 419.19530, 391.24704, 333.15966, 314.12912, 288.11916, 250.13036, 210.10034, 186.008209, 148.10160, 102.09804.

Preparation of mixed copper complex [Cu(L1)(L2)] (3)

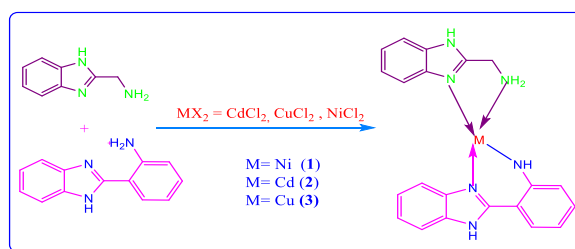
To a solution of anhydrous copper chloride 2.1 g, (8.4 mmol) in 10 mL of ethanol was added a solution of 2-(1*H*-benzimidazol-2-yl) aniline (1.75g, 8.4 mmol) in 10mL of ethanol. The reaction mixture was stirred at room temperature for 30 min and then a solution of 2-aminomethylbenzimidazole (1.23g, 8.4 mmol) in 10 mL of ethanol was added to the mixture

and heated under reflux for 4 h. The progress of reaction was controlled with TLC (DMF/ethanol: 20/80). At the end of the reaction, the reaction mixture was cooled, filtered and the residue washed with ethanol and then with DMF to obtain a dark green precipitate. Mp: 338°C (90% yield) of compound: UV-Vis (DMSO); λ_{\max} (nm): 284; 421. IR (KBr, ν /cm⁻¹) : 3251 (m), 2755 (m), 1667 (m), 1593 (s), 1564 (m), 1521 (s), 1482 (s), 1443 (m), 1412 (s), 1389 (m), 1321(m),1257 (m), 1233 (m), 1120 (m), 1081 (m), 1042 (m), 966 (m), 920 (m), 865 (m), 792 (s), 689(m), 562(m), 523 (m), 441 (m). HRMS (DART-TOF-MS, positive mode) $m/z = (M+H)^+$: 419.19523, 404.22089, 378.07796, 332.24704, 333.10666, 288.12029, 210.09624.

3. Results and Discussion

3.1-Chemistry

Our approach started with the synthesis of mixed complexes by reacting one equivalent ethanolic solution of 2-(2-aminophenyl)-1-*H*-benzimidazole (L1), one equivalent of metal salt (MX₂) in the same solvent ethanol and one equivalent of 2-aminomethylbenzimidazole (L2) in ethanol (Scheme 1). All newly obtained complexes were fully characterized by spectroscopic data of FT-IR, high-resolution mass spectrometry (HRMS), UV-Visible electronic absorption, thermal analysis, and X-ray powder diffraction studies.



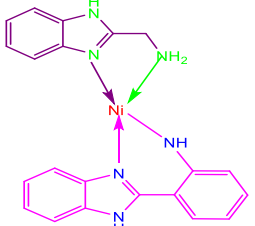
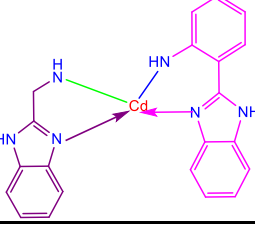
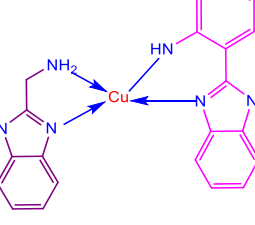
Scheme 1: Synthesis of mixed complexes

Table 1: Analytical data of synthesized complexes

Mass spectra of organonickel complex reproduced in figure 2, reveals that the structure is tetrahedral. This structure was established essentially by molecular ion peak situated at $m/z = 414.30206$ (calcd. 414.10974) attributed to $[M+H]^+$. Also, the spectra display the presence of another peak due to $[(M+H)-CH_3-NH_3]^+$ at $m/z = 382.22057$ (calcd. 382.05972) assigned to the loss of methylammonium motif from molecular fragments $[M+H]^+$. The basic fragment at $m/z = 210.10052$ (calcd. 210.10257) was associated with ligand fragment $L1H^+$. These data

confirm also that the nickel atom is linked with

The infrared data of mixed complexes and both

Entry	Complex	Colour	Empirical formula	Yield (%)	Mp(°C)
1		Pale Green	C ₂₁ H ₁₈ N ₆ Ni	88	> 350
2		white	C ₂₁ H ₁₈ N ₆ Cd	85	233
3		Dark Green	C ₂₁ H ₁₈ N ₆ Cu	90	338

Ligand **L1** and coordinated first with ligand **L2** by the amino as well as the azomethine group of both ligands **L1** and **L2**. Concerning the cadmium complex; mass spectrometry data indicate also a tetrahedral structure. The mass spectrum of organocadmium presented in [figure 3](#), manifest the presence of molecular ion peak (M+Na)⁺ at m/z = 490.04405. The structure was also confirmed by the first fragment at m/z = 459.22685 (calcd. 459.09816) corresponding to benzimidazol-cyclohexylamine linked to cadmium metal and phenylethane-1,2-diamine. The second fragment at m/z = 333.15966 (calcd. 333.06378) associated with the ammonium aniline motif connected to cadmium metal and cyclohex-2-ene-1,2-diamine. The basic peak at m/z = 210.10034 (calcd. 210.10257) was attributed to ligand L1H⁺. The pic at m/z = 148.10160 (calcd. 148.08692) is associated with L2H⁺. These results prove the formation of the complex and the structure described above proposes that the coordination of the cadmium has been provided by the amino groups of both ligands and also by the azomethine groups.

free ligands **L1**, **L2** were collected in [table 2](#). The important infrared bands relatively to metal complexes and their ligands were analyzed and examined, along with their provisional assignments. For example, we presented in [figure 4](#), the IR spectra of organonickel complex.

These results manifest, for all complexes that the chlorine atoms are a good leaving group and they have undergone the nucleophilic attacks of the amino group as well as the azomethine group of both ligand **L1** and **L2**.

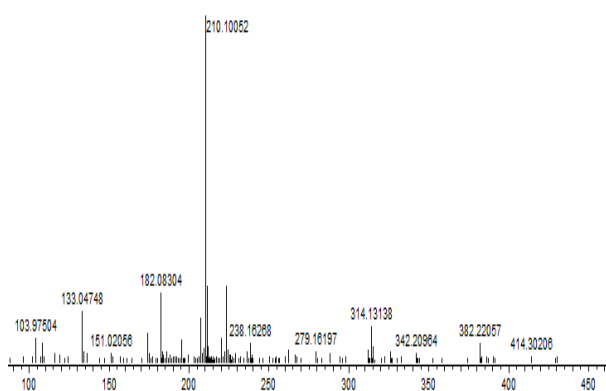


Figure 2: Mass Spectra of organonickel complex

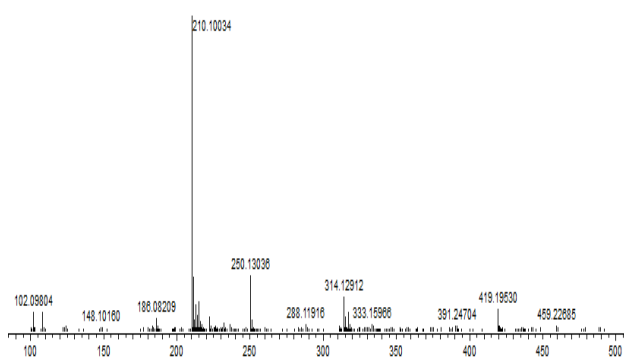


Figure 3: Mass Spectra of organocadmium complex

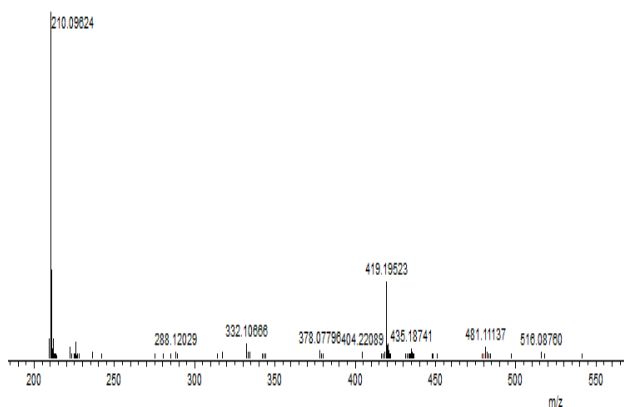


Figure 4: Mass Spectra of organocopper complex

These results manifest, for all complexes that the chlorine atoms are a good leaving group and they have undergone the nucleophilic attacks of the amino group as well as the azomethine group of both ligand L1 and L2.

The infrared data of mixed complexes and both free ligands L1, L2 were collected in table 2. The important infrared bands relatively to metal complexes and their ligands were analyzed and examined, along with their provisional assignments. For example, we presented in figure 4, the IR spectra

of organonickel complex. Regarding the IR results, it has been revealed that the ligands L1 and L2 have a principle peak of absorption respectively at $\nu = 3384$ and 3376 cm^{-1} attributed to $\nu(\text{NH}_2)$. The same band is not observed in the infrared spectra of both complexes Ni (II) and Cu(II) which indicates the establishment of M-N band with the ligands L1 and L2 and respectively Ni (II) and Cu(II) metal and confirm the formation of coordination complexes.

The cadmium complex shows the presence of this band but it is shifted towards the low frequencies and displays a broad spectrum at 3379 cm^{-1} indicating the implication of the amino group of each ligand in the coordination.

In appreciation, C=N stretching frequencies of azomethine motif emerged at 1576 cm^{-1} for ligand L1 and 1580 cm^{-1} for ligand L2, which varies in the complexes and passes at lower frequencies (1571 , 1593 cm^{-1}) respectively for a metal complex of Ni (II) and Cu (II), this is in good agreement with a previously reported data [47,48]. However, this band shifted slightly for the higher frequency at 1609 cm^{-1} for the cadmium complex.

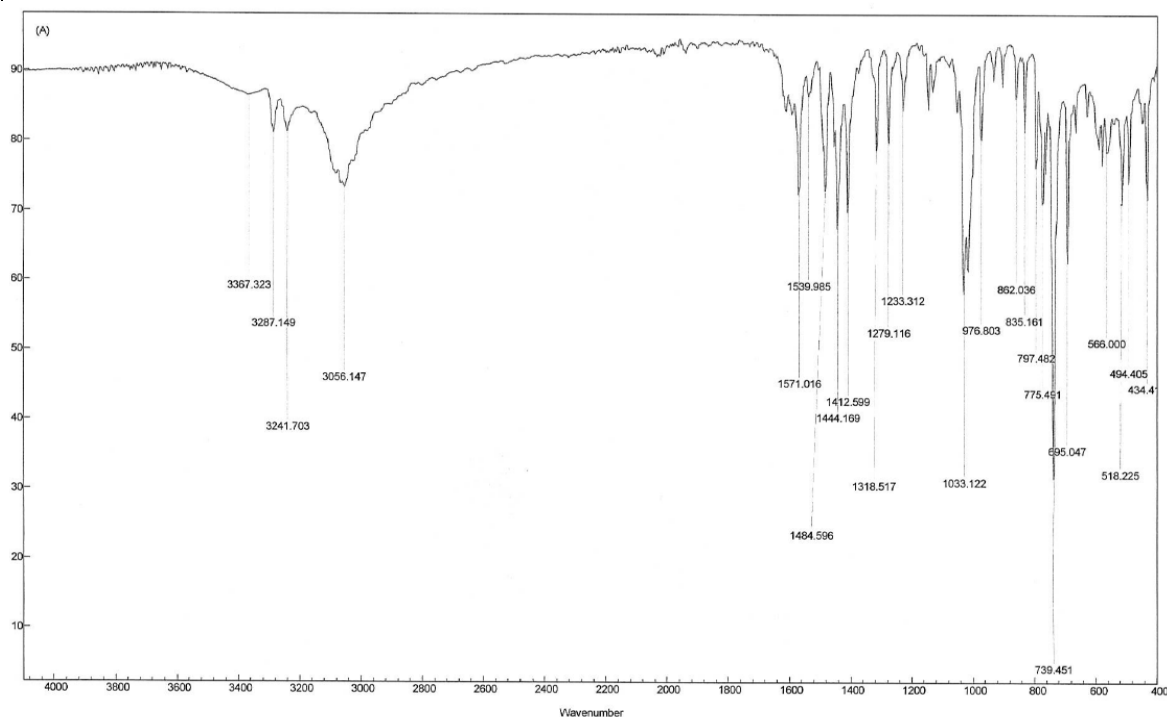
The presence of new bands at 434 , 435 , and 441 cm^{-1} respectively for Ni (II), Cd (II), and Cu (II) is a further sign of the coordination of ligands with metal ions complex and assigned respectively to metal-nitrogen M-N [49]. These bands were absent in ligands spectra, thus confirming the participation of the nitrogen atoms in the coordination.

The UV-Vis absorption of different ligands and their complexes was achieved in DMSO at room temperature and the result was resumed in Table 3. Free ligand L1 show respectively three transitions at 209 , 242 nm attributed to $\pi \rightarrow \pi^*$ band and third transition at 335 nm relatively to $n \rightarrow \pi^*$ band. Moreover, the ligand L2 presents also three bands, two of them appear at 236 and 290 nm assigned to $\pi \rightarrow \pi^*$ transition and a third band located at 407 nm attributed to $\pi(\text{N}) \rightarrow d$ transition. Organocadmium complex revealed the presence of two transitions, first at 287 nm corresponding to $\pi \rightarrow \pi^*$ and the second transition at 353 nm assigned to $\pi \rightarrow \pi^*$ band, different than those of free ligands L1 and L2, this indicates the coordination of both ligands to metal cadmium.

Moreover, organonickel complex spectra present also two transitions, one of them at 288 nm assumed to $\pi \rightarrow \pi^*$ in UV domain and at 352 nm appeared a second transition assigned to $n \rightarrow \pi^*$ band confirm the formation of the complex via the coordination of ligands to metal.

Table 2: The vibrational assignment wavenumbers in cm^{-1} of ligands L1, L2 and their mixed complexes

Complex	$\nu(\text{NH}_2)$		$\nu(\text{N-H})_{\text{benzim}}$ (ligands)	$\nu(\text{N-H})_{\text{benzim}}$ (complex)	$\nu(\text{C=N})$	$\nu(\text{M-N})$ (complex)
L1	3384	3366	3201	-	1576	-
L2	3376	3340	3245	-	1580	-
[Ni(L1)(L2)]	-	3285	-	3240	1571	434
[Cd(L1)(L2)]	3379	-	-	3174	1609	435
[Cu(L1)(L2)]	-	3251	-	-	1593	441

**Figure 5: IR spectra of organonickel mixed complex [Ni(L1)(L2)]****Table 3. The electronic data of free ligands and their mixed complexes**

Compound	λ_{max} (nm)	ν (cm^{-1})	Assignment
L1	209	47846	$\pi \rightarrow \pi^*$
	242	41322	$\pi \rightarrow \pi^*$
	335	29850	$n \rightarrow \pi^*$
L2	236	42372	$\pi \rightarrow \pi^*$
	290	34482	$\pi \rightarrow \pi^*$
	407	24570	$\pi(\text{N}) \rightarrow d$
[Cd(L1) (L2)]	287	34843	$\pi \rightarrow \pi^*$
	353	28328	$n \rightarrow \pi^*$
[Ni(L1) (L2)]	288	34722	$\pi \rightarrow \pi^*$
	352	28409	$n \rightarrow \pi^*$
[Cu(L1) (L2)]	284	35211	$\pi \rightarrow \pi^*$
	421	23752	$(y^2) {}^3A_2g(F) \rightarrow {}^3T_1g(F)$

The thermogram degradation of organonickel complex Ni (II) will be described and reveals the presence of two endothermic decomposition stages. The first endothermic stage at 365°C is responsible for the desorption of *o*-phenyldiamine with mass loss amounting to 22.40 (calcd. 22.41). The second step (endothermic) in the range of 383-415 °C is assigned to the elimination of chlorine atom with a mass loss amounting to 6.46% (calcd. 7.33 %).

The thermal decomposition of the Ni (II) complex showed two endothermic stages at 52-250 and 395 °C. The first step is attributed to the exclusion of two chlorine atom with a mass loss of 13.00% (calculated 13.19%). The second step is attributed to the removal of an aniline group with a mass loss of 16.95% (calculated 17.10%).

Copper thermograph complex visualized an endothermic stage at 181-272°C corresponding to the detachment of an aniline group. The second endothermic step in the range 275-399 °C associated

to desorption of benzimidazole and chlorine atom with a mass loss amounting to 32.06 (calcd. 31.52%).

The X-ray powder diffraction was realized to determine the crystalline system type, lattice parameters; interaxial angles, cell volume, crystallinity size, and density. From the listed data, the elementary cell parameters were also calculated and reassembled in table 4. The X-ray powder diffraction results of the compounds affirmed that the Cu (II) complex has a triclinic structure, Cd (II) complex possess a triclinic structure and Ni (II) complex occupy a rhombohedral structure. Moreover, using the diffraction data, the average crystallite sizes of the complexes, *D*, were calculated according to the Scherrer equation ($D = K\lambda / \beta \cos\theta$), where *K* is the form factor and λ is the length. X-ray waveform (1.5406 Å), θ is the Bragg diffraction angle, and is the total mid-height width of the diffraction peak) [50,51]. The average crystallite sizes of all the samples were found to be 152-185 nm.

Table 4: X-ray powder diffraction crystal data of complexes: Lattice constant, interaxial angle, crystal system, unit cell volume, 2 θ range, crystallinity size and density

Parameters		[Cu (L1)(L2)]	[Ni(L1)(L2)]	[Cd(L1)(L2)]
Empirical formula		C ₂₁ H ₁₈ N ₆ Cu	C ₂₁ H ₁₈ N ₆ Ni	C ₂₁ H ₁₈ N ₆ Cd
Lattice constant	a (Å)	8.330	16.813	12.20
	b (Å)	9.321	16.813	12.20
	c (Å)	9.518	16.813	5.426
Inter axial angle	α (°)	108.84	90.000000	90.000000
	β (°)	98.66	90.000000	90.000000
	γ (°)	114.91	90.000000	120.000000
Crystal system		a \neq b \neq c, $\alpha\neq\beta\neq\gamma$	a \neq b \neq c, $\alpha=\gamma=90, \beta\neq90$	a \neq b \neq c, $\alpha=\beta=90 ;\gamma=120$
		Triclinic	Rhombohedral	Hexagonal
Unit cell Volume (Å ³)		598.0	4753	699
2 θ range		10.63-54.52	10.463-68.049	10.085-71.5
Crystallite Size		420	191	363
Density (gcm ⁻³)		1.704	3.468	2.540

3.2. Biology

3.2.1. Bioactivity score evaluation

The prediction of the bioactivity scores of Ni(II), Cu(II) and Cd(II) complexes were obtained by analyzing their bioactivity scores of GPCR (G-protein coupled receptors ligand), KI (kinase inhibitor), PI (protease inhibitor), EI (enzyme inhibitor), ICM (ion channel modulator) and NRL (nuclear receptor ligand). This study was performed with molinspiration software [52]. From the results

depicted in table 5, Ni(II), Cu(II) and Cd(II) complexes exhibited good bioactivity given by GPCR ligand, moderately nuclear receptor ligand, ion channel modulator, and kinase inhibitor. The tested compounds possess similar bioactivity scores as compared to aspirin for all drug targets.

Table 5. The prediction of the bioactivity scores of Ni(II), Cu(II) and Cd(II) complexes

Complex	GPCR Ligand	Enzyme inhibitor	Nuclear Receptor ligand	Protease inhibitor	Ion channel Modulator	Kinase Inhibitor
Ni(II)	-0.20	0.03	-0.40	-0.12	0.09	0.04
Cu(II)	0.20	0.15	-0.18	-0.04	0.15	0.31
Cd(II)	0.08	0.05	-0.12	-0.09	0.06	0.14
Aspirin	-0.76	-0.28	-0.44	-0.82	-0.32	-1.06

Table 6: Toxicity Model Report of Cu(II) complex

Classification	Target	Shorthand	Prediction	Probability
Organ toxicity	Hepatotoxicity	dili	Inactive	0.56
Toxicity end points	Carcinogenicity	carcino	Inactive	0.60
Toxicity end points	Immunotoxicity	immuno	Inactive	0.65
Toxicity end points	Mutagenicity	mutagen	Inactive	0.59
Toxicity end points	Cytotoxicity	cyto	Inactive	0.61
Tox21-Nuclear receptor signalling pathways	Androgen Receptor (AR)	nr_ar	Inactive	0.93
Tox21-Nuclear receptor signalling pathways	Androgen Receptor Ligand Binding Domain (AR-LBD)	nr_ar_lbd	Inactive	0.91
Tox21-Nuclear receptor signalling pathways	Aromatase	nr_aromatase	Inactive	0.81
Tox21-Nuclear receptor signalling pathways	Estrogen Receptor Alpha (ER)	nr_er	Inactive	0.72
Tox21-Nuclear receptor signalling pathways	Estrogen Receptor Ligand Binding Domain (ER-LBD)	nr_er_lbd	Inactive	0.91
Tox21-Nuclear receptor signalling pathways	Peroxisome Proliferator Activated Receptor Gamma (PPAR-Gamma)	nr_ppar_gamma	Inactive	0.88
Tox21-Stress response pathways	Nuclear factor (erythroid-derived 2)-like 2/antioxidant responsive element (nrf2/ARE)	sr_are	Inactive	0.85
Tox21-Stress response pathways	Heat shock factor response element (HSE)	sr_hse	Inactive	0.85
Tox21-Stress response pathways	Mitochondrial Membrane Potential (MMP)	sr_mmp	Inactive	0.79
Tox21-Stress response pathways	Phosphoprotein (Tumor Suppressor) p53	sr_p53	Inactive	0.85
Tox21-Stress response pathways	ATPase family AAA domain-containing protein 5 (ATAD5)	sr_atad5	Inactive	0.80

3.2.2. Prediction toxicity of mixed complexes

The theoretical toxicity study of different new complexes has been achieved based on program protox-II-prediction toxicity of chemicals [53]. The results of this study revealed that all target compounds exhibited no significant toxicity to all human cells. For example, we present in the following, the results obtained from the prediction toxicity of the copper II mixed complex in table 6.

4. Conclusion

New mixed complex derived from 2-aminomethylbenzimidazole, 2-(1*H*-Benzimidazol-2-

yl) aniline and metal chloride Cd (II), Ni(II) and Cu(II) was successfully achieved. IR results of the metal complexes confirmed that the coordination of the ligands to the metal ions via nitrogen atoms. The structure of different complexes was established with mass spectrometry and mentioned that it has a tetrahedral structure. The X-ray powder diffraction data suggest that the Cu (II) complex has a triclinic structure, Cd (II) complex occupies a triclinic structure and Ni (II) complex occupy a rhombohedral structure. The bioactivity score of tested compounds possesses a similar as compared to aspirin for all drug targets. The results of the theoretical toxicity study of different new complexes have been achieved based on program protox-II-prediction toxicity of chemicals

and revealed that all target compounds exhibited no significant toxicity to all human cells.

Declaration of conflict interest:

The authors acknowledge that there is no any conflict of interest in this work.

Acknowledgements

This work is supported by the Department of Chemistry, College of Sciences, Qassim University . The author thanks Dr. Fahd M. Almenderej for the realization of DTA-DTG, IR and UV-Vis spectra.

References

- Gatadia S., Madhavia Y.V., Choprab S., Nanduria S., Promising antibacterial agents against multidrug resistant *Staphylococcus aureus*, *Bioorganic Chemistry*, **92**, 103252 (2019).
- Mishra R. V., Ghanavatkar C. W. , Malib S. N., Qureshi S. I. , Chaudhari H. K., Sekara N., Design, synthesis, antimicrobial activity and computational studies of novel azo linked substituted benzimidazole, benzoxazole and benzothiazole derivatives. *Computational Biology and Chemistry.*, **78**, 330 (2019).
- Song D., Shutao M., Recent development of benzimidazole-containing antibacterial agents, *ChemMedChem*, **11** (7), 646 (2016).
- Karaburun A. Ç. G., soglu B. K. Ç., Çevik U. A., Osmaniye D., Sa glik B. N., Levent S., Özkay Y., Atlı Ö., Koparal A. S. , Kaplancıklı Z. A., Synthesis and antifungal potential of some novel benzimidazole-1, 3, 4-oxadiazole compounds, *Molecules*, **24** (1), 191 (2019).
- Rathore A., Ahsan R. S. M. J., Ali A., Subbarao N., Jadav S. S., Umar S., ShaharYar M., In vivo anti-inflammatory activity and docking study of newly synthesized benzimidazole derivatives bearing oxadiazole and morpholine rings, *Bioorganic Chemistry*, **70**, 107 (2017).
- Moneer A. A., Mohammed K.O., El-Nassan H. B., Synthesis of Novel Substituted Thiourea and Benzimidazole Derivatives Containing a Pyrazolone Ring as Anti-Inflammatory Agents, *Chemical Bioogy & Drug Design*, **87**(5), 784 (2016).
- Mavrova A. T., Anichina K. K., Vuchev D. I., Tsenov J. A., Denkova P. S., Kondeva M. S., Micheva M. K., Antihelminthic activity of some newly synthesized 5 (6)-(un) substituted-1H-benzimidazol-2-ylthioacetyl piperazine derivatives, *European Journal Medicinal Chemistry* **41**(12), 1412 (2006).
- Keri R. S., Rajappa C. K., Patil S. A., Nagaraja B. M., Benzimidazole-core as an antimycobacterial agent *Pharmacological Reports*, **68** (6), 1254 (2016).
- Yadav, S., Lim, S. M., Ramasamy, K., Vasudevan, M., Shah, S. A. A., Mathur, A., & Narasimhan, B.. Synthesis and evaluation of antimicrobial, antitubercular and anticancer activities of 2-(1-benzoyl-1H-benzo [d] imidazol-2-ylthio)-N-substituted acetamides. *Chemistry Central Journal*, **12**(1), 66 (2018).
- Kuo H. L., Lien J. C., Chung C. H., Chang C. H., Lo S. C, Tsai I. C., Peng H. C., Kuo S. C., Huang T. F., Naunyn-Schmiedeberg's, NP-184 [2-(5-methyl-2-furyl) benzimidazole], a novel orally active antithrombotic agent with dual antiplatelet and anticoagulant activities. *Naunyn-Schmiedeberg's archives of pharmacology*, **381**(6), 495 (2010).
- Abida N., Neelum Q., Humaira N., Arif-ullah K., Rehan P., Fawad A., Adil S., Synthesis, characterization, anti-ulcer action and molecular docking evaluation of novel benzimidazole-pyrazole hybrids *Chemistry Central Journal*, **11**(1), 1 (2017).
- Shaharyar M., Mazumder A., Benzimidazoles: A biologically active compounds, Benzimidazoles: A biologically active compounds, *Arabian Journal of Chemistry*, **10**, 157 (2017).
- Tonellia M. , Gabriele E., Piazzab F., Basilicoc N., Parapinid S., Tasso B., Loddoe R., Sparatorea F., Sparatore A., Benzimidazoles: A biologically active compounds. *Journal Enzyme Inhibition Medicinal. Chemistry*, **33** (1), 210 (2018).
- Kankala S., Kankala R., Gundepaka P., Thota N., Nerella S., Gangula M., Guguloth H., Kagga M., Vadde R., Vasam C. Regioselective synthesis of isoxazole–mercaptobenzimidazole hybrids and their in vivo analgesic and anti-inflammatory activity studies, *Bioorganic Medicinal Chemistry Letters*, **23** (5), 1306 (2013).
- Sharma D., Narasimhan B., Kumar P., Judge V., Narang R., Clercq E. D., J. Balzarini, Regioselective synthesis of isoxazole–mercaptobenzimidazole hybrids and their in vivo analgesic and anti-inflammatory activity studies, *Journal Enzyme Inhibition Medicinal Chemistry*, **24** (5), 1161 (2009).
- Yoon Y. K., Ali M. A., Wei A. C., Choon T. S., Ismail R., Synthesis and evaluation of antimycobacterial activity of new benzimidazole aminoesters, *European Journal Medicinal Chemistry*, **93**, 614 (2015).
- Miller J. F., Turner E. M., Gudmundsson K. Jenkinson S., S., Spaltenstein A., Thomson M., Wheelan P., N-substituted benzimidazole CXCR4 antagonists as potential anti-HIV agents, *Bioorganic Medicinal Chemistry. Letters*, **20**,

- 2125 (2010).
18. Singh I., Luxami V., Paul K., Synthesis and in vitro evaluation of naphthalimide–benzimidazole conjugates as potential antitumor agents. *Organic Biomolecular Chemistry*, **17** (21), 5349 (2019).
 19. P. Naik, P. Murumkar, R. Giridhar, M. R. Yadav, Angiotensin II receptor type 1 (AT1) selective nonpeptidic antagonists-A perspective, *Bioorganic Medicinal Chemistry*, **18**, 8418 (2010)
 20. Marcus A. J. , Iezhitsa I., Agarwal R., Vassiliev P., Spasov A., O. Zhukovskaya, V. Anisimova, N. M. Ismail, Intraocular pressure-lowering effects of imidazo [1, 2-a]-and pyrimido [1, 2-a] benzimidazole compounds in rats with dexamethasone-induced ocular hypertension, *European. Journal Pharmacology*, **850**, 75 (2019).
 21. Monforte A., Rao A., Logoteta P., Ferro S., Luca L. D., Barreca M.L., Iraci N., Maga G., Clercq E.D., Pannecouque C., Chimirri A., Novel N1-substituted 1, 3-dihydro-2H-benzimidazol-2-ones as potent non-nucleoside reverse transcriptase inhibitors. *Bioorganic Medicinal Chemistry*, **16** (15), 7429 (2008).
 22. Tsay S., Hwu J.R., Singha R., Huang W., Chang Y.H., Hsu M., Shieh F., Lin C., Hwang K.C., Horng J., Clercq E.D., Vliegen I., Neyts J. Coumarins hinged directly on benzimidazoles and their ribofuranosides to inhibit hepatitis C virus. *European Journal Medicinal Chemistry*, **63**, 290 (2013).
 23. Sahoo B. M., Banik B. K., Rao N. S., Raju B., Microwave Assisted Green Synthesis of Benzimidazole Derivatives and Evaluation of Their Anticonvulsant Activity. *Current Microwave Chemistry*, **6**(1), 23 (2019).
 24. Khan F., Nadeem S., Anti-ulcerogenic effect of 2-(pyrimidinylsulfinyl) benzimidazole derivative against different ulcerogenic agents in rats. *Pharmacologyonline* **2**, 1217 (2011).
 25. Sharma M. C., Kohli D.V., Sharma S., Synthesis and biological evaluation of some new benzimidazoles derivatives 4'-(5-amino-2-[2-substituted-phenylamino)-phenyl-methyl]-benzimidazol-1ylmethyl)-biphenyl-2-carboxylic acid: Nonpeptide angiotensin II receptor antagonists. *International Journal. Drug. Delivery.*, **2**(3), 265 (2010).
 26. Mrabti N. N., Elhallaoui M., QSAR study and molecular docking of benzimidazole derivatives as potent activators of AMP-activated protein kinase, *Journal Taibah University for Science*, **11**(1), 18 (2017).
 27. Sharma M. C. , QSAR studies of novel 1-(4-methoxyphenethyl)-1H-benzimidazole-5-carboxylic acid derivatives and their precursors as antileukaemic agent, *Journal Taibah University for Science.*, **10**(1), 122 (2016).
 28. Bhati S, Kumar V, Singh S, Singh J. Synthesis, Characterization, Antimicrobial, Anti-tubercular, Antioxidant Activities and Docking Simulations of Derivatives of 2-(pyridin-3-yl)-1H-benzo [d] imidazole and 1, 3, 4-Oxadiazole Analogy. *Letters in Drug Design & Discovery*. 2020;17:000-.
 29. Goud N. S. r, Ghouse S. M., Vishnu J., Komal D., Talla V., Alvala R., Pranay J., Kumar J., Qureshi I. A., Alvala M. , Synthesis of 1-benzyl-1H-benzimidazoles as galectin-1 mediated anticancer agents, *Bioorganic Chemistry*, **89**, 103016 (2019).
 30. Wang M. , Wu Y. , Xu C. , Zhao R. , Huang Y. , Zeng X. , Chen T. f. , Design and Synthesis of 2-(5-Phenylindol-3-yl) benzimidazole Derivatives with Antiproliferative Effects towards Triple-Negative Breast Cancer Cells by Activation of ROS-Mediated Mitochondria Dysfunction, *Chemistry-an Asian Journal.*, **14**(1), 2648 (2019).
 31. Bansal Y., Silakari O., The therapeutic journey of benzimidazoles: a review. *Bioorganic Medicinal Chemistry*, **20**(21), 6208 (2012).
 32. Mahmood K., Hashmi W., Ismail H.,Mirza B., Wamley B. T., Akhter Z., Rozas I., Baker R. J. , Synthesis, DNA binding and antibacterial activity of metal (II) complexes of a benzimidazole Schiff base. *Polyhedron*, **157**, 326 (2019).
 33. Cota I., Marturano V. , Tylkowski B. , Ln complexes as double faced agents: Study of antibacterial and antifungal activity. *Coordination Chemistry Reviews*, **396**, 49 (2019).
 34. Wang X. , Ling N. , Che Q.-T. , Zhang Y.-W. , Yang H.-X. , Ruan Y., Zhao T.-T. , Synthesis, structure and biological properties of benzimidazole-based Cu (II)/Zn (II) complexes. *Inorganic Chemistry Communication*, **105**, 97 (2019).
 35. Bharti N., Garza M.G., Cruz-Vega D.E., Castro-Garza J., Saleem K., Naqvi F., Maurya M.R., Azam A., Synthesis, characterization and antiamebic activity of benzimidazole derivatives and their vanadium and molybdenum complexes. *Bioorganic Medicinal Chemistry Letters*, **12**(6), 869 (2002).
 36. Lim Y., Lu L., Zhum M., Wang Q., Yuan C., Xing S., Fu X., Mei Y., Potent inhibition of protein tyrosine phosphatases by copper complexes with multi-benzimidazole derivatives,

- BioMetals, 24(6), 993 (2011).
37. Toro P., Klahn A. H., Pradines B., Lahoz F., Pascual A., Biot C., Arancibia R., Potent inhibition of protein tyrosine phosphatases by copper complexes with multi-benzimidazole derivatives. *Inorganic Chemistry Communication*, 35, 126 (2013).
 38. Aljhdali M., Synthesis, characterization and equilibrium studies of some potential antimicrobial and antitumor complexes of Cu (II), Ni (II), Zn (II) and Cd (II) ions involving 2-aminomethyl benzimidazole and glycine. *Spectrochimica Acta Part A: Molecular and Biomolecular Spectroscopy*, 112, 364 (2013).
 39. Natha M., Sainia P. K., Kumar A., Synthesis, structural characterization, biological activity and thermal study of tri-and diorganotin (IV) complexes of Schiff base derived from 2-aminomethyl benzimidazole. *Applied Organometallic Chemistry*, 23 (11), 434 (2009).
 40. Kumaravel G., Utthra P. P., Raman N., Exploiting the biological efficacy of benzimidazole based Schiff base complexes with l-Histidine as a co-ligand: Combined molecular docking, DNA interaction, antimicrobial and cytotoxic studies. *Bioorganic Chemistry*, 77, 269 (2018).
 41. El-Sherif A. A., Synthesis and characterization of some potential antitumor palladium(II) complexes of 2-aminomethylbenzimidazole and amino acids, *Journal. Coordination Chemistry*, 64(12), 2035 (2011).
 42. Ajani O. O., Tolu-Bolaji O. O., Olorunshola S. J., Zhao Y., Aderohunmu D. V., Structure-based design of functionalized 2-substituted and 1,2-disubstituted benzimidazole derivatives and their in vitro antibacterial efficacy *Journal Advanced Research*, 8(6),703 (2017).
 43. Paul A., Gupta R. K.r, Dubey M., Sharma G., Koch B., Hunda G., Hundal M. S., Pandey D. S., Potential apoptosis inducing agents based on a new benzimidazole schiff base ligand and its dicopper (II) complex, *RSC Advances*, 4(78), 41228 (2014).
 44. Paul A., S. Anbu, G. Sharma, M. L. K., B. Kochm, M. Fátima C. G. da Silva, A. J. L. Pombeiro, Synthesis, DNA binding, cellular DNA lesion and cytotoxicity of a series of new benzimidazole-based Schiff base copper(ii) complexes, *Dalton Transaction*, 44 (46), 19983 (2015).
 45. Tang L., Cai M., A highly selective and sensitive fluorescent sensor for Cu²⁺ and its complex for successive sensing of cyanide via Cu²⁺ displacement approach, *Sensors and Actuators B: Chemical* 173, 862 (2012).
 46. Mukhopadhyay, S., Gupta, R. K., Biswas, A., Kumar, A., Dubey, M., Hundal, M. S., Pandey, D. S., A dual-responsive "turn-on" bifunctional receptor: a chemosensor for Fe³⁺ and chemodosimeter for Hg²⁺, *Dalton Transaction*, 44(16), 7118 (2015).
 47. Mohan S., Sundaraganesan N., FTIR and Raman studies on benzimidazole, *Spectrochimica Acta Part (A)*, 47(8), 1111 (1991).
 48. Sundaraganesan N., Ilakiamani S., Subramani P., Dominic Joshua B., Comparison of experimental and ab initio HF and DFT vibrational spectra of benzimidazole, *Spectrochimica Acta Part A*, 67(3-4), 628 (2007).
 49. Hill D. G., Rosenberg A. F., Comparison of experimental and ab initio HF and DFT vibrational spectra of benzimidazole, *The journal Chemical Physics*, 24 (6), 1219 (1956).
 50. Baranwal B. P., Fatma T., Varma A., Synthesis, spectral and thermal characterization of nano-sized, oxo-centered, trinuclear carboxylate-bridged chromium(III) complexes of hydroxycarboxylic acids, *Journal Molecular Structure*, 920 (1-3), 472 (2009).
 51. Kolmas J., Jaklewicz A., Zima A., Bucko M., Paszkiewicz Z., Lis J., Sloarczyk A., Kolodziejcki W., Incorporation of carbonate and magnesium ions into synthetic hydroxyapatite: The effect on physicochemical properties *Journal Molecular Structure* 987 (1-3), 40 (2011).
 52. Thangarasu P., Selvi S.T., Manikandan A., Unveiling novel 2-cyclopropyl-3-ethynyl-4-(4-fluorophenyl) quinolines as GPCR ligands via PI3-kinase/PAR-1 antagonism and platelet aggregation valuations; development of a new class of anticancer drugs with thrombolytic effects *Bioorganic chemistry*, 81, 468 (2018).
 53. Banerjee P., Eckert A. O., Schrey A. K., Preissner R., ProTox-II: a webserver for the prediction of toxicity of chemicals *Nucleic Acids Research*, 46 (W1), 257(2018).